Available online at www.sciencedirect.com
ScienceDirect
Neuroscience Letters 411 (2007) 200–205
Neuroscience Letters
www.elsevier.com/locate/neulet

PET imaging with [^{11}C]PBR28 can localize and quantify upregulated peripheral benzodiazepine receptors associated with cerebral ischemia in rat

Masao Imaizumi [a,*], Hyun-Ju Kim [b], Sami S. Zoghbi [a], Emmanuelle Briard [a], Jinsoo Hong [a], John L. Musachio [a], Christl Ruetzler [c], De-Maw Chuang [b], Victor W. Pike [a], Robert B. Innis [a], Masahiro Fujita [a]

[a] *Molecular Imaging Branch, National Institute of Mental Health, National Institutes of Health, Building 1, Room B3-10, 1 Center Drive, MSC 0135, Bethesda, MD 20892-0135, USA*
[b] *Molecular Neurobiology Section, National Institute of Mental Health, National Institutes of Health, Bethesda, MD, USA*
[c] *Stroke Branch, National Institute of Neurological Disorders and Stroke, National Institutes of Health, Bethesda, MD, USA*

Received 12 July 2006; received in revised form 2 September 2006; accepted 7 September 2006

Abstract

Peripheral benzodiazepine receptors (PBRs) are upregulated on activated microglia. We recently developed a promising positron emission tomography (PET) ligand, [^{11}C]PBR28, with high affinity and excellent ratio of specific to nonspecific binding. We assessed the ability of [^{11}C]PBR28 PET to localize PBRs in a rat permanent middle cerebral artery occlusion (MCAO) model of neuroinflammation. [^{11}C]PBR28 was intravenously administered to rats at 4 and 7 days after permanent MCAO. In all experiments, arterial blood was sampled for compartmental modeling of regional distribution volumes, and rat brains were sampled after imaging for *in vitro* [^{3}H]PK 11195 autoradiography and histological evaluation. [^{11}C]PBR28 PET and [^{3}H]PK 11195 autoradiography showed similar areas of increased PBRs, especially in the peri-ischemic core. Results from these in vivo and in vitro methods were strongly correlated. In this first study to demonstrate neuroinflammation *in vivo* with small animal PET, [^{11}C]PBR28 had adequate sensitivity to localize and quantify the associated increase in PBRs.
Published by Elsevier Ireland Ltd.

Keywords: Peripheral benzodiazepine receptor; Neuroinflammation; Small animal PET; Cerebral ischemia; Activated microglia

Although the peripheral benzodiazepine receptor (PBR) was initially discovered in organs such as kidney and lung, it was later identified in the central nervous system [16]. PBR is distinct from the central benzodiazepine allosteric site that is associated with $GABA_A$ receptors. In normal conditions, PBR is expressed in low levels in some neurons and glial cells. PBR can be a clinically useful marker to detect neuroinflammation, because activated microglial cells in inflammatory areas express much greater levels of PBR than those in resting conditions [1].

PBR has been imaged with positron emission tomography (PET) using [*N*-methyl-^{11}C]1-(2-chlorophenyl-*N*-methylpropyl)-3-isoquinoline carboxamide (PK 11195), either as racemate or (*R*)-enantiomer. However, a low ratio of specific to nonspecific binding may limit its sensitivity to detect therapeutic interventions. Its relatively high lipophilicity ($c\log P = 5.3$) may have caused high nonspecific binding in brain [9]. We developed a new radioligand, *N*-acetyl-*N*-(2-[^{11}C]methoxybenzyl)-2-phenoxy-5-pyridinamine ([^{11}C]PBR28) which showed much greater specific signal than [^{11}C]PK 11195 in nonhuman primates [3]. PBR28 is a close analog of [methoxy-^{11}C](*N*-5-fluoro-2-phenoxyphenyl)-*N*-(2,5-dimethoxybenzyl)acetamide (DAA1106) developed by Zhang et al. [19] and that was used to localize neuroinflammation with *in vitro* tissue sections [10]. The purpose of this study was to determine whether increased PBRs in a rat permanent middle cerebral artery occlusion (MCAO) model could be measured *in vivo* with [^{11}C]PBR28 and a small animal PET scanner. If successful in this model, [^{11}C]PBR28 could be used to explore the pathophysiology of neuroinflammation associ-

* Corresponding author. Tel.: +1 301 451 5014; fax: +1 301 480 3610.
E-mail address: imaizumim@intra.nimh.nih.gov (M. Imaizumi).

0304-3940/$ – see front matter. Published by Elsevier Ireland Ltd.
doi:10.1016/j.neulet.2006.09.093

ated with human disorders such as cerebral ischemia, multiple sclerosis, Alzheimer's disease, and Parkinson's disease.

All procedures were performed in compliance with Guide for Care and Use of Laboratory Animals. Details of the surgical procedures for rat permanent MCAO model are described previously [15]. Animals were anesthetized with 3% halothane in a mixture of 30% O_2 and 70% NO_2, and a 4-0 nylon suture with a silicon-coated tip was inserted from the left external carotid artery to the left internal carotid artery and then to the Circle of Willis to occlude the origin of the left middle cerebral artery.

N-Acetyl-*N*-(2-methoxybenzyl)-2-phenoxy-5-pyridinamine [11] has moderate lipophilicity ($c\log P = 2.98$) and high affinity for PBR ($IC_{50} = 0.6$ nM measured *versus* [^{3}H]PK 11195). Selectivity of PBR28 was screened at 10 μM and found to have <50% displacement of the target radioligand for the following receptors: 11 subtypes of serotonin receptor, 8 subtypes of adrenergic receptor, 4 subtypes of dopamine receptor, 4 subtypes of histamine receptor, 2 subtypes of muscarinic cholinergic receptor, and dopamine, norepinephrine, and serotonin transporters. As expected, PBR28 showed $K_i > 10$ μM for several central benzodiazepine receptor subtypes (*i.e.*, $GABA_A$ receptor). PBR28 was labeled by ^{11}C-methylation of the *O-desmethyl* precursor [3]. The specific radioactivity of [^{11}C]PBR28 at the time of injection was 59.7 ± 2.7 GBq/μmol with this and subsequent data expressed as mean ± S.D.

Four male Sprague–Dawley rats with permanent MCAO (239 ± 66 g) were used under 1–1.5% isoflurane anesthesia. At 4 and 7 days after permanent MCAO, two bolus and two bolus plus infusion (B/I) studies were performed with arterial blood sampling. Details of the experimental procedures are described previously [5]. PET data were acquired with the Advanced Technology Laboratory Animal Scanner (ATLAS).

In two bolus studies with 120 min scan, [^{11}C]PBR28 (activity: 47 and 53 MBq) was injected intravenously over 6 min. B/I experiments were acquired with two different bolus to infusion ratios (B/I = 2 and 5 h). The bolus portion of the activity was administered over 3 min, after which the pump administered the remaining activity at a constant rate over 150 min. In total, the animals received 185 and 259 MBq from the bolus and infusion components. PK 11195 (10 and 20 mg/kg, i.v.) was administered at 60 min to measure specific binding.

In all experiments, arterial blood samples were collected in heparin-coated tubes (Thomas Scientific, Swedesboro, NJ, USA) eight times between 0 and 10 min and at 20, 40, 60, 90, 120, and 150 min. The volume was 100 μL for the initial eight samples and 200 μL for the last samples. Body temperature was maintained by a heating pad and monitored with a rectal temperature probe.

PET images were reconstructed with a 3D ordered subset expectation maximization algorithm, achieving 1.7 mm full-width at half maximum resolution [17]. Image data were not corrected for attenuation or scatter. Head movements were corrected using Statistical Parametric Mapping2 (SPM2, Wellcome Department of Cognitive Neurology, London, UK), and an average image was created from all realigned images. Within the resolution of the PET images, we visually identified the approximate level of the coronal section relative to an atlas of the rat brain [13]. We then visually selected the autoradiographic and histological sections corresponding to the PET tomograph. Regions of interest were manually placed over the ischemic core, peri-ischemic core, and contralateral side on the averaged PET images based on morphological changes in stained histological sections. Brain uptake of radioactivity was decay corrected to injection time and expressed as percent standard uptake value (%SUV), which normalizes for injected activity and body weight.

$$\%\mathrm{SUV} = \left[\frac{\text{activity per gram tissue}}{\text{injected activity}}\right] \times \text{gram body weight} \times 100$$

Plasma samples were mixed with acetonitrile containing reference PBR28. Distilled water was added and mixed well. Total radioactivity in this solution was measured with a calibrated gamma counter. Deproteinized plasma samples were centrifuged at $10{,}000 \times g$ for 1 min to remove denatured proteins. The supernatant was then analyzed directly by reversed phase high-performance liquid chromatography (HPLC). The percent recovery of radioactivity in the supernatant was calculated relative to that in the precipitate.

As described previously [5], total distribution volume (V'_T) was measured by obtaining arterial input function with 60 min data before displacement in each experiment and by applying nonlinear least-squares fitting with an unconstrained two-compartment model using PMOD 2.65. The standard errors of nonlinear least-squares fit were determined from the covariance matrix and expressed as a percentage of the value estimation relative to the estimated values (coefficient of variation, %COV).

Rats were decapitated after PET imaging, and the brains were quickly removed, frozen in powdered dry ice, and stored at −70 °C until sectioning. Cryostat sections (20 μm thick) were thaw-mounted onto poly-L-lysine coated glass slides (Sigma–Aldrich, Natick, MA, USA). PBRs were labeled with [^{3}H]PK 11195 (PerkinElmer Life and Analytical Sciences Inc., Boston, MA, USA, specific activity 71.1 Ci/mmol; 1.0 mCi/mL), using a methodology adapted from the literature [7]. Total binding was determined with 1 nM [^{3}H]PK 11195, and nonspecific binding was determined on consecutive sections in the presence of excess (20 μM) unlabeled PK 11195. Tissue sections and calibrated tritium scales (Amersham Biosciences Inc., Piscataway, NJ, USA) were opposed to a ^{3}H imaging plate (TR2025, Fujifilm, Stamford, CT, USA) for 7 days. Images were analyzed with Multi Gauge® (ver. 3.0, Fujifilm).

For a histological evaluation, serial frozen sections (20 μm thick) were stained with 0.5% cresyl violet, dehydrated through graded alcohols (75, 95, and100%), dipped in xylene, and coverslipped.

Correlation was assessed with the Pearson correlation coefficients. All statistical tests were considered significant at $P < 0.05$. SPSS 12.0 (SPSS Inc., Chicago, IL, USA) was used for statistical analyses.

Histological sections confirmed that the cerebral artery occlusion caused brain ischemia (Fig. 1C). The core of the ischemic lesion showed poor cresyl violet staining and consisted of loose necrotic tissue with partial cavitation (panel 3 in Fig. 1D). The

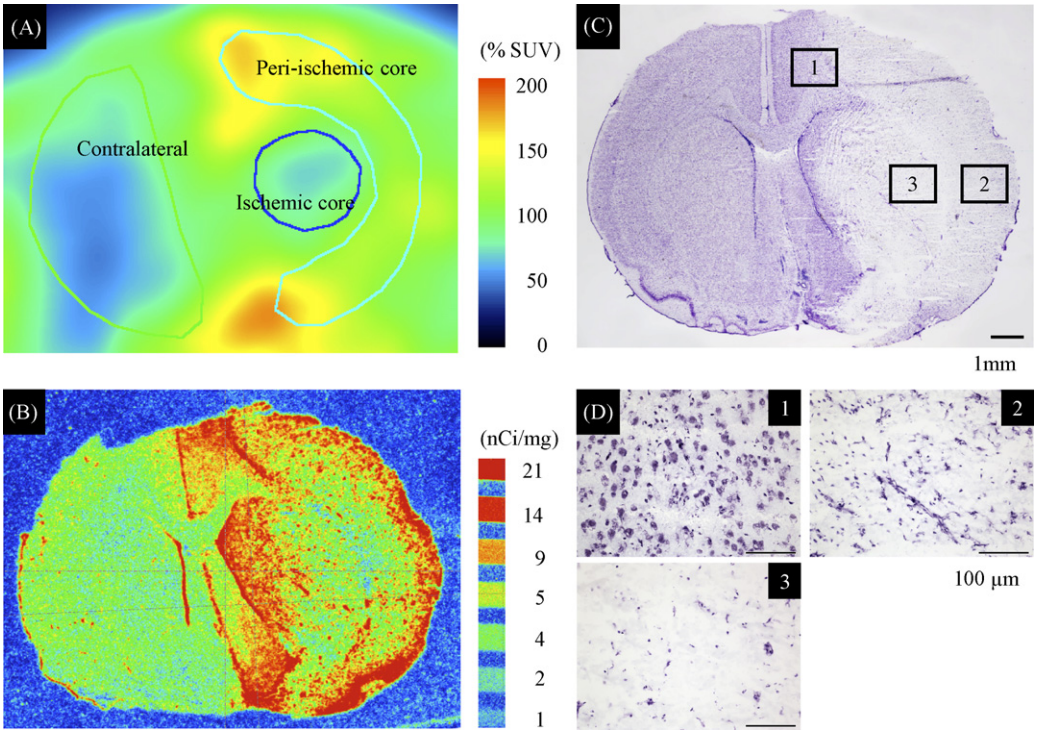

Fig. 1. (A) [^{11}C]PBR28 PET average image (bolus #2). (B) [^{3}H]PK 11195 autoradiogram. (C) Cresyl violet staining of coronal brain section (bar = 1 mm). (D) Magnification of cresyl violet staining displaying morphological changes within the ischemic lesion and in the perifocal area (bar = 100 μm in panels 1–3). Panel 1: perifocal area showing increased cellular survival with selective neuronal necrosis. Panel 2: cortex (layers 1 and 2) with some preservation of cellular elements, which consist of mostly microglia and microvessels. Panel 3: the ischemic core consisting of loose necrotic tissue with partial cavitation. Visual localizations of PBRs were similar between [^{11}C]PBR28 *in vivo* image and *in vitro* [^{3}H]PK 11195 autoradiogram. Both [^{11}C]PBR28 PET image and [^{3}H]PK 11195 autoradiogram showed lower activity in the ischemic core than in peri-ischemic core.

superficial layers of the cortex (layers 1 and 2) showed some preserved cellular elements which consisted mostly of microglia and microvessels. Staining in the perifocal area (*i.e.*, the transition area between infarcted and intact tissue) showed greater cellular survival with selective neuronal necrosis (panels 1 and 2 in Fig. 1D). The PET [^{11}C]PBR28 images and [^{3}H]PK 11195 autoradiograms had similar distributions of activity. Both methods showed much higher binding in the peri-ischemic core than in either the ischemic core or the contralateral side (Fig. 1A and B). Because of the limited resolution of PET, the central ischemic region included not only the necrotic core but also surrounding areas that had increased PBR binding (Fig. 1A). Serial PET imaging showed that the peri-ischemic core achieved higher peak levels of activity within 5–10 min of injection and then washed out slower than that in the ischemic core or the contralateral side (Fig. 2).

Radio-HPLC analysis showed two radioactive peaks; one associated with polar radiometabolite and another associated with the parent [^{11}C]PBR28 ligand. Because the increased radioactivity in the ischemic areas was displaced with PK 11195 to the level of the contralateral side (Fig. 3), the increased radioactivity was caused by increased specific binding but not by increased levels of radioactive metabolites. To examine the receptor specificity of brain uptake, we displaced the radioli-

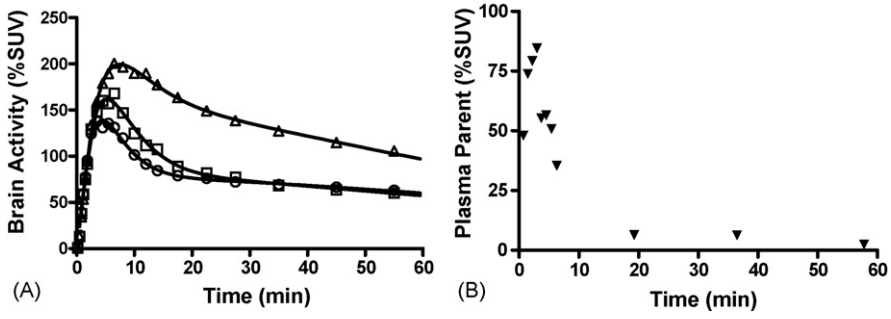

Fig. 2. (A) Brain activity, two-compartmental fitting, and (B) [^{11}C]PBR28 concentrations in plasma. Following a bolus injection of 53 MBq (bolus #2), regional brain activities were measured with PET and arterial plasma [^{11}C]PBR28 concentrations were measured with HPLC analysis. [^{11}C]PBR28 showed high peak uptake of approximately 140, 170, and 200% SUV in the contralateral side, the ischemic core and the peri-ischemic core, respectively. Solid lines show fitting by an unconstrained two-tissue compartment model. (△) Peri-ischemic core; (□) ischemic core; (◯) contralateral; (▼) plasma parent.

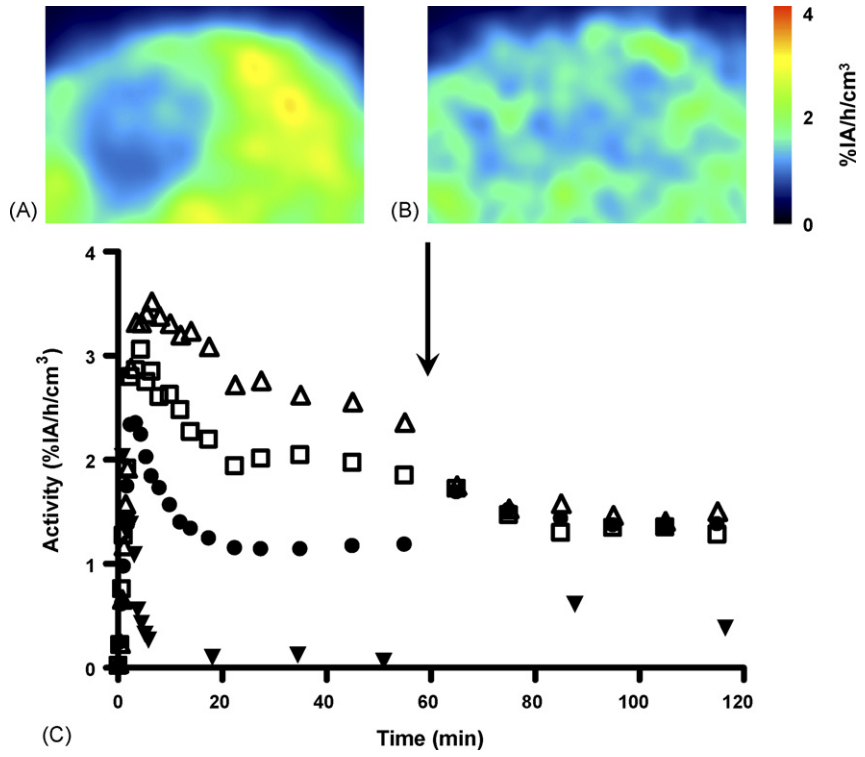

Fig. 3. Bolus and infusion experiment with displacement (10 mg/kg PK 11195). [^{11}C]PBR28 PET average images before displacement (30–60 min) (A) and after displacement (90–120 min) (B), and time–activity curves during the experiment (C). After the administration of PK 11195, activity on ischemic and contralateral sides showed identical levels indicating that the increased activity in the ischemic areas was exclusively caused by increased specific binding of [^{11}C]PBR28. The *y*-axis is expressed as %injected activity/h/cm^3. (△) Peri-ischemic core; (□) ischemic core; (●) contralateral; (▼) plasma parent.

gand with the structurally dissimilar agent PK 11195 during a B/I study (Fig. 3). Because equilibrium was not achieved within the time frame of the PET experiments, one experiment with B/I = 5 h (Fig. 3) and the other with B/I = 2 h showed decreasing and increasing brain activity, respectively. Nevertheless, in both of these experiments, the administration of PK 11195 reduced activity in the peri-ischemic core and ischemic core region to that in the contralateral side. Thus, the increased activity in the peri-ischemic core was specific (displaceable) binding to PBRs. Injection of PK 11195 consistently caused a marked increase in the plasma concentration of [^{11}C]PBR28 (Fig. 3), probably by displacing the radioligand from peripheral organs like lung and kidney. Thus, PK 11195 displaced activity in the peri-ischemic core in brain despite a higher concentration of [^{11}C]PBR28 in plasma.

V'_T was measured in all experiments except one B/I experiment with significant undershoot, in which brain activity continued to increase prior to the injection of PK 11195. Because a one-compartment model showed poor fitting, we used a two-compartment model, and V'_T was well identified with COV < 15%. These V'_T values were shown in Table 1 with specific binding measured by autoradiography. Compared to contralateral side, the ischemic core and peri-ischemic core showed 100–190 and 140–290% increases, respectively (Table 1). The peri-ischemic core/contralateral and ischemic core/contralateral ratios obtained from the V'_T by the two-compartment model were significantly correlated with those from [^{3}H]PK 11195 autoradiograms (Fig. 4).

To our knowledge, this is the first *in vivo* study to visualize PBRs induced by neuroinflammation using small animal PET. In previous studies, ^{3}H- and ^{11}C-labeled PK 11195 were used to localize PBRs with *in vitro* autoradiography [8] and *in vivo* PET imaging [6,12], respectively. Autoradiography was successful, because the radioligand was directly applied to the tissue and much of the nonspecific binding was washed from the slide-mounted tissue sections. The PET radioligand [^{11}C]PK

Table 1
PET distribution volume and autoradiographic measurement of PBRs

	Bolus #1		Bolus #2		Bolus and infusion	
	PET V'_T (mL/cm^3)	Autoradiogram specific binding (nCi/mg tissue)	PET V'_T (mL/cm^3)	Autoradiogram specific binding (nCi/mg tissue)	PET V'_T (mL/cm^3)	Autoradiogram specific binding (nCi/mg tissue)
Contralateral	21.5	1.5	13.5	2.3	12.6	0.6
Ischemic core	40.9	3.5	13.0	2.5	19.9	1.7
Peri-ischemic core	61.7	8.3	18.3	6.0	24.3	2.5

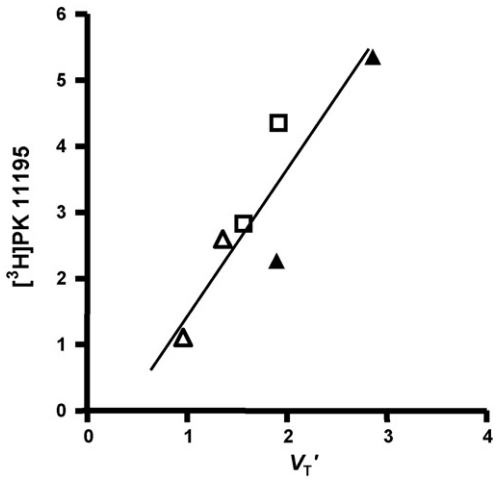

Fig. 4. Comparison between [11C]PBR28 PET and [3H]PK 11195 autoradiographic measurements. The *X* and *Y* axes of the graph are shown as ratios of peri-ischemic core and ischemic core to the contralateral sides. $y = 2.11x - 0.61$, $R^2 = 0.80$, $P < 0.05$. (▲) Bolus #1; (△) bolus #2; (□) bolus and infusion.

11195 has been used to localize PBRs associated with ischemic stroke in human subjects [6,12,14]. The new ligand [11C]PBR28 showed that as much as 80–90% of total binding was specific in normal rhesus monkeys (in preparation). Such a high proportion of specific binding should provide high sensitivity to visualize an increase in PBRs even in small rat brain and also to detect changes in humans by therapeutic interventions. The increased [11C]PBR28 brain uptake in ischemic areas was exclusively caused by increased specific binding and not by other factors such as changes in nonspecific uptake or cerebral blood volume, because PK 11195 displaced the uptake in two B/I experiments (Fig. 3). Complete equilibrium was not achieved in these experiments due to the slow kinetics of the radioligand. Nevertheless, complete displacement occurred in both experiments.

The arterial occlusion used in this study clearly altered cerebral blood flow. Nevertheless, the PET imaging results are not merely artifacts of this altered flow, since the postmortem autoradiograms confirmed increased PBR binding. Furthermore, the compartmental modeling method with arterial input function is designed to minimize the effects of regional variations in blood flow. Finally, the B/I method reached nearly stable equilibrium values, which would be independent of blood flow and were displaceable. Nevertheless, the PET images showed some apparent mismatch relative to the autoradiograms. For example, the autoradiograms showed more dense PBRs in the area medial to infarct than appeared in the PET image (Fig. 1A and B). The compartmental modeling method showed apparent stability and, thus, independence of flow in relatively large regions of interest. Smaller regions (like that medial to ischemic lesion) may require longer times to reach equilibrium and may not have done so during the scanning session.

In this study, we measured the density of PBRs with both V'_T and a ratio to a reference region (the contralateral side). V'_T represents the ratio at equilibrium of concentration of radiotracer in brain to that in plasma. V'_T is vulnerable to numerous errors in measurement, including quantitation of the concentration of radioligand in small plasma samples and separation of parent tracer from radiometabolites. Furthermore, V'_T is vulnerable to fluctuation in plasma free fraction, which was not measured in this study. In a similar way, the ratio to a reference region is also vulnerable to variations in specific and nonspecific binding in the reference region. Additional studies are required to determine whether a distribution volume or a reference tissue measurement is more reliable.

The distribution of the increased PBR detected in the current study matched what was reported by *in vitro* measurement of PBR and PET in nonhuman primates and humans. *In vitro* [3H]PK 11195 autoradiography following MCAO in the rodent showed increased binding in peri-ischemic areas [2,8]. [11C]PK 11195 uptake increased not only within but also around the ischemia following MCAO in baboons [18], with similar preliminary findings in stroke patients [6]. Previous *in vitro* studies reported increases of PBR at the time point when the current study was performed. The increases was detected on day 3 after cerebral ischemia and reached to maximal levels after 7 days, which closely parallels the histologically detected accumulation of activated microglia [2,4]. The increase of PBR binding in ischemic and peri-ischemic areas has been interpreted as presenting a microglial activation [2,4]. Our results agree with the prior reports. Thus, the increased [11C]PBR28 binding presumably reflects the inflammatory response of microglia or astrocytes associated with the ischemic damage. Finally, *in vivo* PET imaging with [11C]PBR28 can localize and quantify increased PBRs associated with inflammation surrounding cerebral infarction in rat. [11C]PBR28 is a promising radioligand to measure neuroinflammation in man.

Acknowledgements

We thank John M. Hallenbeck for histological evaluation; Michael Green and Jurgen Seidel who built the rodent PET camera; Jeih-San Liow for processing PET data; and PMOD group for providing PMOD 2.65. This research was supported by the Intramural Program of NIMH (Project #Z01-MH-002795-04).

References

[1] R.B. Banati, Neuropathological imaging: *in vivo* detection of glial activation as a measure of disease and adaptive change in the brain, Br. Med. Bull. 65 (2003) 121–131.

[2] J. Benavides, C. Capdeville, F. Dauphin, A. Dubois, D. Duverger, D. Fage, B. Gotti, E.T. MacKenzie, B. Scatton, The quantification of brain lesions with an omega 3 site ligand: a critical analysis of animal models of cerebral ischaemia and neurodegeneration, Brain Res. 522 (1990) 275–289.

[3] E. Briard, J. Hong, J.L. Musachio, S.S. Zoghbi, M. Fujita, M. Imaizumi, V. Cropley, R.B. Innis, V.W. Pike, Synthesis and evaluation of two candidate 11C-labeled radioligands for brain peripheral benzodiazepine receptors, J. Label. Compd. Radiopharm. 48 (2005) S71.

[4] A. Dubois, J. Benavides, B. Peny, D. Duverger, D. Fage, B. Gotti, E.T. MacKenzie, B. Scatton, Imaging of primary and remote ischaemic and excitotoxic brain lesions. An autoradiographic study of peripheral type benzodiazepine binding sites in the rat and cat, Brain Res. 445 (1988) 77–90.

[5] M. Fujita, S.S. Zoghbi, M.S. Crescenzo, J. Hong, J.L. Musachio, J.Q. Lu, J.S. Liow, N. Seneca, D.N. Tipre, V.L. Cropley, M. Imaizumi, A.D. Gee,

J. Seidel, M.V. Green, V.W. Pike, R.B. Innis, Quantification of brain phosphodiesterase 4 in rat with (R)-[^{11}C]Rolipram-PET, Neuroimage 26 (2005) 1201–1210.

[6] A. Gerhard, J. Schwarz, R. Myers, R. Wise, R.B. Banati, Evolution of microglial activation in patients after ischemic stroke: a [^{11}C](R)-PK11195 PET study, Neuroimage 24 (2005) 591–595.

[7] R. Grossman, E. Shohami, A. Alexandrovich, I. Yatsiv, Y. Kloog, A. Biegon, Increase in peripheral benzodiazepine receptors and loss of glutamate NMDA receptors in a mouse model of closed head injury: a quantitative autoradiographic study, Neuroimage 20 (2003) 1971–1981.

[8] J. Katchanov, C. Waeber, K. Gertz, A. Gietz, B. Winter, W. Bruck, U. Dirnagl, R.W. Veh, M. Endres, Selective neuronal vulnerability following mild focal brain ischemia in the mouse, Brain Pathol. 13 (2003) 452–464.

[9] A. Lockhart, B. Davis, J.C. Matthews, H. Rahmoune, G. Hong, A. Gee, D. Earnshaw, J. Brown, The peripheral benzodiazepine receptor ligand PK11195 binds with high affinity to the acute phase reactant alpha1-acid glycoprotein: implications for the use of the ligand as a CNS inflammatory marker, Nucl. Med. Biol. 30 (2003) 199–206.

[10] J. Maeda, T. Suhara, M.R. Zhang, T. Okauchi, F. Yasuno, Y. Ikoma, M. Inaji, Y. Nagai, A. Takano, S. Obayashi, K. Suzuki, Novel peripheral benzodiazepine receptor ligand [^{11}C]DAA1106 for PET: an imaging tool for glial cells in the brain, Synapse 52 (2004) 283–291.

[11] A. Nakazato, Japanese Patent 001476 (2000).

[12] S. Pappata, M. Levasseur, R.N. Gunn, R. Myers, C. Crouzel, A. Syrota, T. Jones, G.W. Kreutzberg, R.B. Banati, Thalamic microglial activation in ischemic stroke detected *in vivo* by PET and [^{11}C]PK11195, Neurology 55 (2000) 1052–1054.

[13] G. Paxinos, C. Watson, The Rat Brain in Stereotaxic Coordinates, fourth ed., Academic Press, 1998.

[14] C.J. Price, D. Wang, D.K. Menon, J.V. Guadagno, M. Cleij, T. Fryer, F. Aigbirhio, J.C. Baron, E.A. Warburton, Intrinsic activated microglia map to the peri-infarct zone in the subacute phase of ischemic stroke, Stroke 37 (2006) 1749–1753.

[15] M. Ren, V.V. Senatorov, R.W. Chen, D.M. Chuang, Postinsult treatment with lithium reduces brain damage and facilitates neurological recovery in a rat ischemia/reperfusion model, Proc. Natl. Acad. Sci. U.S.A. 100 (2003) 6210–6215.

[16] H. Schoemaker, M. Bliss, H.I. Yamamura, Specific high-affinity saturable binding of [^{3}H] R05-4864 to benzodiazepine binding sites in the rat cerebral cortex, Eur. J. Pharmacol. 71 (1981) 173–175.

[17] J. Seidel, J. Vaquero, M.V. Green, Resolution uniformity and sensitivity of the NIH ATLAS small animal PET scanner: comparison to simulated LSO scanners without depth-of-interaction capability, IEEE Trans. Nuclear Sci. 50 (2003) 1347–1350.

[18] G. Sette, J.C. Baron, A.R. Young, H. Miyazawa, I. Tillet, L. Barre, J.M. Travere, J.M. Derlon, E.T. MacKenzie, *In vivo* mapping of brain benzodiazepine receptor changes by positron emission tomography after focal ischemia in the anesthetized baboon, Stroke 24 (1993) 2046–2057, discussion 2057–8.

[19] M.R. Zhang, T. Kida, J. Noguchi, K. Furutsuka, J. Maeda, T. Suhara, K. Suzuki, [^{11}C]DAA1106: radiosynthesis and *in vivo* binding to peripheral benzodiazepine receptors in mouse brain, Nucl. Med. Biol. 30 (2003) 513–519.